RESEARCH ARTICLE

Role of microRNA-195 in cardiomyocyte apoptosis induced by myocardial ischaemia–reperfusion injury

CHANG-KUI GAO[1]*, HUI LIU[2], CHENG-JI CUI[3], ZHAO-GUANG LIANG[4], HONG YAO[4] and YE TIAN[4]

[1]*Department of Emergency, Longnan Hospital of Daqing, Daqing 163001, People's Republic of China*
[2]*Department of Clinical Laboratory, Women and Children Hospital of Qingdao, Qingdao 266000, People's Republic of China*
[3]*Department of Nephrology, the Affiliated Hospital to Changchun University of Chinese Medicine, Changchun 130000, People's Republic of China*
[4]*Department of Laboratory, The First Hospital of YanTai, YanTai 261400, People's Republic of China*

Abstract

This study aims to investigate microRNA-195 (miR-195) expression in myocardial ischaemia–reperfusion (I/R) injury and the roles of miR-195 in cardiomyocyte apoptosis though targeting Bcl-2. A mouse model of I/R injury was established. MiR-195 expression levels were detected by real-time quantitative PCR (qPCR), and the cardiomyocyte apoptosis was detected by TUNEL assay. After cardiomyocytes isolated from neonatal rats and transfected with miR-195 mimic or inhibitor, the hypoxia/reoxygenation (H/R) injury model was established. Cardiomyocyte apoptosis and mitochondrial membrane potential were evaluated using flow cytometry. Bcl-2 and Bax mRNA expressions were detected by RT-PCR. Bcl-2, Bax and cytochrome c (Cyt-c) protein levels were determined by Western blot. Caspase-3 and caspase-9 activities were assessed by luciferase assay. Compared with the sham group, miR-195 expression levels and rate of cardiomyocyte apoptosis increased significantly in I/R group (both $P < 0.05$). Compared to H/R + negative control (NC) group, rate of cardiomyocyte apoptosis increased in H/R + miR-195 mimic group while decreased in H/R + miR-195 inhibitor group (both $P < 0.05$). MiR-195 knockdown alleviated the loss of mitochondrial membrane potential ($P < 0.05$). MiR-195 overexpression decreased Bcl-2 mRNA and protein expression, increased BaxmRNA and protein expression, Cyt-c protein expression and caspase-3 and caspase-9 activities (all $P < 0.05$). While, downregulated MiR-195 increased Bcl-2 mRNA and protein expression, decreased Bax mRNA and protein expression, Cyt-c protein expression and caspase-3 and caspase-9 activities (all $P < 0.05$). Our study identified that miR-195 expression was upregulated in myocardial I/R injury, and miR-195 overexpression may promote cardiomyocyte apoptosis by targeting Bcl-2 and inducing mitochondrial apoptotic pathway.

[Gao C.-K., Liu H., Cui C.-J., Liang Z.-G. Yao H. and Tian Y. 2016 Role of microRNA-195 in cardiomyocyte apoptosis induced by myocardial ischaemia–reperfusion injury. *J. Genet.* **95**, 99–108]

Introduction

Ischaemic heart disease (IHD), a leading cause of mortality, accounts for substantial long-term morbidity worldwide (Moran *et al.* 2014). Therapeutic strategy for IHD, currently is timely reperfusion of the occluded artery; on the other hand, reperfusion may lead to myocardial ischaemia–reperfusion (I/R) injury (Frank *et al.* 2012; Hausenloy and Yellon 2013). Myocardial I/R injury has been evidenced to have pivotal roles in inducing cardiomyocyte death and left ventricular remodelling, and thus resulting in adverse cardiovascular outcomes, including progressive deterioration of cardiac function, heart failure and death (Frohlich *et al.* 2013; Diez *et al.* 2015). A previous study has documented that improvements of metabolic recovery in cardiomyocytes and mitochondrial-derived oxidative stress are the crucial prevention of myocardial I/R injury (Pisarenko *et al.* 2014). Nevertheless, the mechanisms associated with mitochondrial functions in cardioprotective interventions have not been clearly clarified yet. Therefore, a large number of researchers aim at understanding the potential molecular mechanisms of cardiomyocyte apoptosis and exploring effective therapeutic strategies to ultimately reduce adverse outcomes in myocardial I/R injury (Siddall *et al.* 2013; Dongworth *et al.* 2014; Liu *et al.* 2014). Recently, microRNAs (miRNAs) have been documented to be associated with the regulation of I/R

*For correspondence. E-mail: gaochangkui789@163.com; tianye1013_ty@126.com.

Keywords. microRNA-195; ischaemia–reperfusion; hypoxia/reoxygenation; cardiomyocyte apoptosis; Bcl-2; Bax; Cyt-c; caspase-3; caspase-9; mitochondrial membrane potentia.

injury-induced cardiomyocyte apoptosis and cardiac function, thus emerging as underlying therapeutic agents for myocardial I/R injury (Skommer *et al.* 2014; Di *et al.* 2014).

MiR-195 is characterized by its significant functions in regulating cell cycle, apoptosis, cell metabolism, cell proliferation and metastasis (Yongchun *et al.* 2014; Lei *et al.* 2014; Zhao *et al.* 2014). Recent reports have displayed that miR-195 expression is downregulated in many tumours, such as colorectal cancer, gastric cancer and hepatocellular carcinoma (Liu *et al.* 2010; Wang *et al.* 2013; Deng *et al.* 2013). MiR-195 has been demonstrated to be a tumour repressor in tumourigenesis and may be an underlying target in cancer therapy (Yang *et al.* 2014). Numerous miRNAs play significant regulatory roles in mitochondrial metabolism and mitochondrial pathway is emphasized in the augment of cell apoptosis (Jin and Wei 2014). MiR-195 is identified to be involved in repression of Bcl-2 expression through targeting its 3′-untranslated (3′-UTR) region (Qu *et al.* 2015). Importantly, the role of Bcl-2 in apoptosis pathway is to block Bax-induced apoptosis by suppression of cytochrome c (Cyt-c) releasing from mitochondria (Czabotar *et al.* 2014; Jin *et al.* 2015). The previous literature has ever demonstrated a role of miR-195 in cardiomyocytes, which is regulated through downregulation of Bcl-2 production (Zhu *et al.* 2011). In this study, we established a mouse model of I/R injury to explore the potential roles and mechanisms of miR-195 in cardiomyocyte apoptosis induced by myocardial I/R injury, supplying novel therapeutic strategies for the treatment of myocardial I/R injury.

Materials and methods

Ethics statement

All mice and rats were purchased from Harbin Medical University Laboratorial Animal Center. This animal experiment was conducted in accordance with the recommendations of the Committee for the Purpose of the Control and Supervision of Experiments on Animals (CPCSEA). We made reasonable efforts to minimize the suffering of animals.

Animals and treatments

A total of 30 healthy male C57BL/6 mice (8–10 weeks old) weighing 20–30 g were kept in an environmental room equipped with a constant temperature of 20°C, a humidity of 60% and a programmed 12 h light / 12 h dark cycle for circadian control. All mice were allowed free access to drinking water and sterilized standard diet. The mice were randomly separated into two groups: (i) the sham group ($n = 15$): the mice underwent the sham operation with hearts enlarged and a sutureunder left anterior descending coronary artery (LAD), while without ligation of coronary artery for 150 min; (ii) I/R group ($n = 15$): the mice were treated with the LAD which was reversibly ligated and I/R was induced by 30-min ischaemia followed by 120-min reperfusion.

I/R injury model

All mice were anesthetized with sodium pentobarbital (50 mg/kg) by intraperitoneal injection and fixed for endotracheal intubation by the use of a small animal respirator (60 breaths per min). After removing hair from praecordium, the skin was disinfected with iodine. A longitudinal incision was made from the third to fourth ribs, separating the pectoralis major muscle, serratus anterior muscle and pectoralis minor muscle, and exposing the heart. Then, a 6-0 nylon suture was placed around the l–2 cm of the root of LAD. The suture was loosened after occlusion for 30 min, which was followed by 120 min reperfusion of LAD. Hearts of all mice were then separated and prepared for next experiments. All surgical procedures were carried out under aseptic conditions. The electrocardiogram (ECG) was synchronously recorded until the end of this experiment.

TUNEL assay

The terminal dUTP nick end-labelling (TUNEL) staining was performed with the *in situ* cell death detection kit (Promega, Madison, USA) in accordance with the manufacturer's protocol to detect apoptotic cardiomyocytes. The extracted tissue from mice with I/R model was fixed by 10% formic acid solution. Fixation lasted for 24 h at room temperature. Then, paraffin-embedded specimens were sliced, deparaffinized and dehydrated. After washing with phosphate buffer solution (PBS) twice the sections were blocked in 0.1% Triton X-100 and 0.1% natrium citricum for 15 min. Then the sections were washed in PBS thrice and incubated in 50 μL of TUNEL mix (Roche, Switzerland) containing 0.3 U/mL terminal deoxynucleotidyl transferase and 6.66 mM/mL biotin dUTP in a moist chamber at 37°C for 1.5 h. Nuclei were stained with 5 μg/mL 4′,6-diamidino-2-phenylindole (DAPI) for 5 min at room temperature and observed by fluorescence microscopy.

Cell isolation and culture

Neonatal SD rats (1–2 days old) were disinfected with 75% alcohol, and the hearts were excised and kept in the culture medium. After removing the connective tissue and blood vessels, the hearts were incubated and minced. Then they were transferred into serum bottles supplemented with 4 mL of trypsin / ethylenediaminetetraacetic acid solution at 4°C overnight. After 12–16 h of incubation, 2 mL of Dulbecco's modified Eagle's medium / F12 medium (Invitrogen, Waltham, USA) with 10% foetal bovine serum (FBS) was added into these bottles and transferred into a temperature-controlled oscillator (37°C) for 5 min. Removing the supernatant, 2 mL of collagenase digestion was added into the medium and shaken by oscillator for 1 min. The myocardial tissue after discarding the supernatant and adding 4 mL of collagenase digestion was stirred by a magnetic stirrer for 15 min at 37°C. Cells in the supernatant were centrifuged at 1000 rpm for 5 min. Subsequently, the precipitate was

incubated in 100 nm culture dishes containing 10 mL of DMEM-F12 medium and placed in a humidified 5% CO_2 incubator at 37°C for 70 min, and the supernatant was treated again with centrifugation at 1000 rpm for 5 min. The isolated cardiomyocytes were transferred into the culture medium for culture and purification.

Luciferase reporter gene assay

The Bcl-2 mRNA 3′UTR sequence was amplified by polymerase chain reaction (PCR) and cloned into pGL3-promoterconstruct (Promega), thus obtaining Bcl-23′UTR firefly luciferase reporter gene. The cardiomyocytes were cotransfected with 80 ng Bcl-23′UTR firefly luciferase reporter gene, 40 ng Renilla luciferase reference plasmid pRL-TK and miRNA per controls (final concentration, 20 nM). Twenty-four hours after transfection, the fluorescence activity was detected by a dual-luciferase report gene assay system (Promega). The final data were the ratio of firefly fluorescent value to Renilla fluorescence value.

Cell grouping and transfection

After 5-day culture, cardiomyocytes were randomly divided into five groups: (i) the control group, the cells exposed to normal oxygen; (ii) hypoxia/reoxygenation (H/R) group, the cells exposed to 10 h of hypoxia followed by 2 h of reoxygenation; (iii) H/R + negative control (NC) group, after transfection with negative control oligonucleotides, the cells exposed to 10 h of hypoxia followed by 2 h of reoxygenation; (iv) H/R + miR-195 mimic group, after transfection with miR-195 mimics, the cells exposed to 10 h of hypoxia followed by 2 h of reoxygenation and (v) H/R + miR-195 inhibitor group, after transfection with miR-195 inhibitors, the cells exposed to 10 h of hypoxia followed by 2 h of reoxygenation. The day before transfection, 1×10^5 cells were seeded into six-well plates and in each plate the culture medium with 10% FBS was added. When they reached 50% confluence, miR-195 mimics and miR-195 inhibitors were transfected into each well by applying Lipofectamine 2000 transfection reagent (Invitrogen). Lipofectamine 2000 reagent (5 μL) was diluted into 100 μL OPTI-MEM medium and incubated for 20 min at room temperature. Adding serum free medium into the plates after removing the culture medium, the cells were then incubated for 6 h in an incubator at 37°C. Subsequently, the serum free medium was replaced by the culture medium with 10% FBS to culture cardiomyocytes.

Hypoxia/reoxygenation injury model

Using the model of hypoxia/reoxygenation (H/R) injury, we examined the effect of hypoxia-induced and reoxygenation-induced cell death. After culture medium was removed, the cardiomyocytes were incubated in serum-free DMED without glucose under a hypoxic gas mixture supplemented with 95% N_2 and 5% CO_2, and the medium was placed in a hypoxic incubator (95% N_2 and 5% CO_2) for 10 h which was followed by reoxygenation for 2 h in DMEM containing 10% FBS and glucoseat 37°C in a 5% CO_2 incubator.

Real-time quantitative PCR (qRT-PCR)

Total RNA was isolated by utilizing Trizol reagent (Invitrogen) and the purity and concentration of RNA was detected by UV spectrophotometer. The values of OD260/OD280 of RNA samples were all in normal range (1.8–2.2). The RNA quality was assessed by agarose gel electrophoresis. The cDNA was obtained using One Step PrimeScript® miRNA cDNA Synthesis Kit (Takara, Dalian, China) according to the manufacturer's protocol. The RNU6B was applied as an internal control. The real-time qRT-PCR was carried out by using SYBR® Premix Ex Taq TMII mix according to the manufacturer's protocol. Primer sequences of miR-195 (Takara) were as follow: hsa-miR-195 qPCR primer mix:mature sequence: 5′-U AGC AGCACAGAAAUAUUGGC- 3′. Primer sequences of U6 were: forward primer: 5′-CTCGCTTCGGCAGCA CA-3′, reverse primer: 5′-AACGCTTCACGAATTTGCGT-3′. The reaction mixtures were incubated at 95°C for 30 s, followed by 35–42 cycles of 95°C for 5 s, 55°C for 30 s and 72°C for 30 s. The temperature ranges for the melting curves were: 50–95°C. U6 was applied as an internal control and the $2^{-\Delta\Delta Ct}$ method was applied to determine relative quantitation of miR-195 expression. $\Delta Ct = Ct_{\text{target gene}} - Ct_{U6}, \Delta\Delta Ct = Ct_{\text{experiment group}} - Ct_{\text{control group}}$.

Flow cytometry

The cardiomyocytes were dissociated into single-cell suspension washed in PBS and suspended in 5 μL of AnnexinV-FITC and 5 μL of propidium iodide (PI) solution at room temperature with protection from light. After washing, cells were resuspended in 200 μL of Binding Buffer and stained by 5 μL of AnnexinV-FITC and 5 μL of PI in the dark for 15 min and analysed in flow cytometry by a FACScan (BD FACSCalibur, USA). For detecting mitochondrial membrane potential, cells were stained by Rhodamine 123 (0.1–50 μg /mL) and incubated for 10 min at 37°C in a 5% CO_2 culture medium. After two centrifugation, cells were resuspended in the culture medium for 60 min. The samples (100 μL) were measured on microscope slides (excitation, 488 nm; emission, 515 nm).

Detection of mitochondrial membrane potential

All cells were incubated with 1.0 mM calcein and 25 nM oxidized mitochondrial probe (MitoTracker, Invitrogen). Fluorescence intensity was observed under a fluorescence microscope. Tetramethylrhodamine ethyl ester (TMRE) is a positively charged dye. The enhancement of mitochondrial permeability results in a decrease in membrane potential, inhibiting the accumulation of TMRE, and decreasing the fluorescence value of mitochondrion. And then the cells were incubated with 50 nM TMRE at room temperature for 30 min

and the fluorescence value of TMRE was observed under the fluorescence microscope.

RT-PCR for Bcl-2 and Bax mRNA expression

Total RNA was isolated, cDNA was obtained by reverse transcription and then the PCR amplification was performed. Primer sequences were as follow: Bcl-2 (151 bp):forward primer: 5′-CAACTCCCAATACTGGCTCT-3′, reverse primer: 5′-CGGACTTCGGTCTCCTAAA-3′; GAPDH (299 bp): forward primer:5′-GGGAAACTGTGGCGTGAT-3′, reverse primer: 5′-GAGTGGGTGTCGCTGTTGA-3′; Bax (73 bp): forward primer: 5′-GGCAGACCGTGACCATCTTT-3′, reverse primer: 5′-CCTCAGCCCATCTTCTTCCA-3′. The PCR reaction conditions of Bcl were: predegeneration at 95°C for 5 min, followed by 40 cycles of 95°C for 10 s, 95°C for 15 s, 72°C for 20 s and 82°C for 5 s. PCR reaction conditions of Bax were: predegeneration at 95°C for 5 min, which was followed by 40 cycles of 95°C for 10 s, 59°C for 15 s, 72°C for 20 s and 82°C for 5 s. Standard curve was obtained for total DNA quantification. The relative expression level of target gene in each sample was the concentration of the target gene/ the concentration of *GADPH* gene.

Western blot

The protein concentration of the cardiomyocytes was determined using a BCA protein assay kit. A total of 40 μg protein solution was treated with 10% sodium dodecyl sulphate polyacrylamide gel electrophoresis (SDS-PAGE) and blotted on to polyvinylidenedifluoride (PVDF) membranes, with average pore size of 0.22 μm. Then, the membranes were blocked in 5% nonfat dried milk at room temperature for 1 h and incubated with primary antibodies (1: 500; rabbit antihuman Bax, Bcl-2, and Cyt-c; R&D, Emeryville, USA) at 37°C for 1 h. They were then washed in Tris-buffered saline-Tween 20 (TBST) thrice and incubated with goat antirabbit secondary antibody (1:1000; Dako, USA) at 37°C for 1 h. The scanned images were assessed quantitatively by software IPP6.0 (Media Cybernetics, Bethesda, USA).

Caspase-3 and caspase-9 activity assay

Caspase-3 and caspase-9 activities were assessed using caspase-3 and caspase-9 Activity Assay Kit (BestBio, Shanghai, China). The cardiomyocytes were incubated in the dark for 1–2 h, and these cells were lysed with lysis buffer. Subsequently, caspase-3 and caspase-9 substrates were added to cell lysates and the mixtures were incubated for 2 h at room temperature. The ρNA cleavage rates released from substrates were measured using colorimetric assay kits from the absorbance values at 405 nm and the concentration of ρNA was calculated from a calibration curve.

Statistical analysis

All experimental data were presented as mean ± standard deviation. The SPSS 18.0 software (SPSS, Chicago, USA) was applied for statistical analysis. The *t*-test was applied to compare differences between the two groups. The statistical significance of groups was performed using one-way analysis of variance (ANOVA). Differences with a $P < 0.05$ were determined as statistically significant.

Results

Expression levels of miR-195 in myocardial tissues

The RT-PCR results suggested miR-195 expression level in myocardial tissue of each group, as seen in figure 1. Compared to the sham group, miR-195 expression level in I/R group increased significantly after 30 min ischaemia and 120 min reperfusion ($P < 0.05$).

I/R-induced cardiomyocyte apoptosis

TUNEL assay was utilized to detect the cardiomyocyte apoptosis in myocardial ischaemic region of the Sham group and I/R group (figure 2). The TUNEL-positive cardiomyocytesdid not apparently exist in the sham group. In contrast, the rate of TUNEL-positive cardiomyocytes in I/R group increased significantly (34.5% ± 5.4% versus 2.1% ± 1.5%, $P < 0.05$).

Target gene of miR-195 analysis

The target gene of miR-195 was predicted and screened using the bioinformatics software (Target Scan; http://www.targetscan.org), revealing that the 3′-UTR sequence in Bcl-2 matched miR-195, and a high level of conservation existed among different species (figure 3a). Compared with the control group, miR-195 inhibited the luciferase activity of Bcl-2 3′UTR firefly luciferase reporter gene while it had no effect on the luciferase activity of target site deleted mutated reporter gene (figure 3b). Therefore, miR-195 inhibited reporter

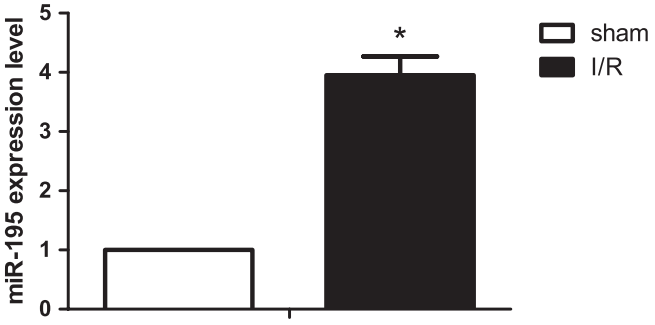

Figure 1. Comparison of miR-195 expression levels between the sham group and the I/R group. MiR-195, miRNA-195; I/R, ischaemia-reperfusion;*, compared with the sham group, $P < 0.05$.

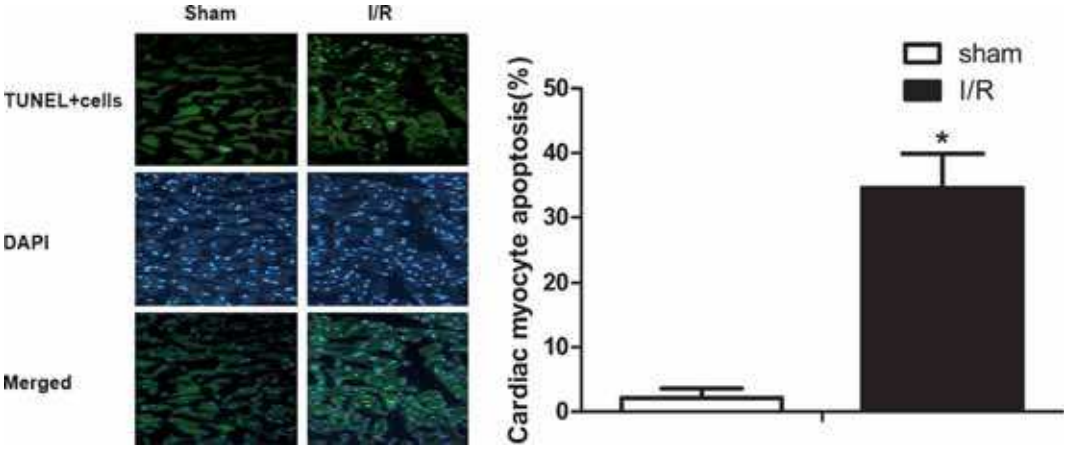

Figure 2. TUNEL assay testing I/R-induced cardiomyocyte apoptosis in the sham group and the I/R group (× 200). I/R, ischaemia–reperfusion; *compared with the sham group, $P < 0.05$; nucleus of apoptotic cardiomyocytes were issued by green fluorescence, all nucleated cells stained with DAPI were issued by blue fluorescence.

gene activity of target gene through complementation fixation with target gene Bcl-2 and target sequence 3′-UTR.

Expression levels of miR-195 after transfection

Real-time qPCR detecting the expression levels of miR-195 after transfection showed that miR-195 expression levels in the H/R group and the H/R + NC group increased apparently as compared with the control group (both $P < 0.05$). There was no obvious difference in the expression levels of miR-195 between the H/R group and the H/R + NC group ($P > 0.05$). Compared with the H/R + NC group, miR-195 expression levels in the H/R + miR-195 mimic group increased significantly ($P < 0.05$); while miR-195 expression levels in the H/R + miR-195 inhibitor group decreased obviously ($P < 0.05$) (figure 4).

Effect of miR-195 overexpression on H/R-induced cardiomyocyte apoptosis

The apoptosis rate of cardiomyocytes was 1.98 ± 0.15% in control group, 12.75 ± 0.46% in H/R group, and 13.02 ± 0.59% in H/R +NC group, suggesting that cell apoptosis rate in the control group was apparently lower than the H/R group and H/R + NC group (both $P < 0.05$) and that H/R injury could stimulate apoptosis rate of cardiomyocytes (as shown in figure 5). When compared with H/R + NC group, the rate of cardiomyocyte apoptosis in H/R + miR-195 mimic group and H/R + miR-195 inhibitor group were 18.65 ± 1.48% and 6.56 ± 1.06%, respectively. The apoptosis rate in H/R + miR-195 mimic group was markedly increased but decreased in H/R + miR-195 inhibitor group (both $P < 0.05$).

Effect of miR-195 overexpression on mitochondrial membrane potential

Mitochondrial membrane permeabilization is related to the loss of mitochondrial membrane potential. Figure 6 represents the loss of mitochondrial membrane potential induced by H/R injury in H/R and H/R + NC groups was significantly increased compared to control group (both $P < 0.05$). In addition, the loss of mitochondrial membrane potential was enhanced by miR-195 overexpression in H/R + miR-195 mimic group than in H/R + NC group ($P < 0.05$), but the loss

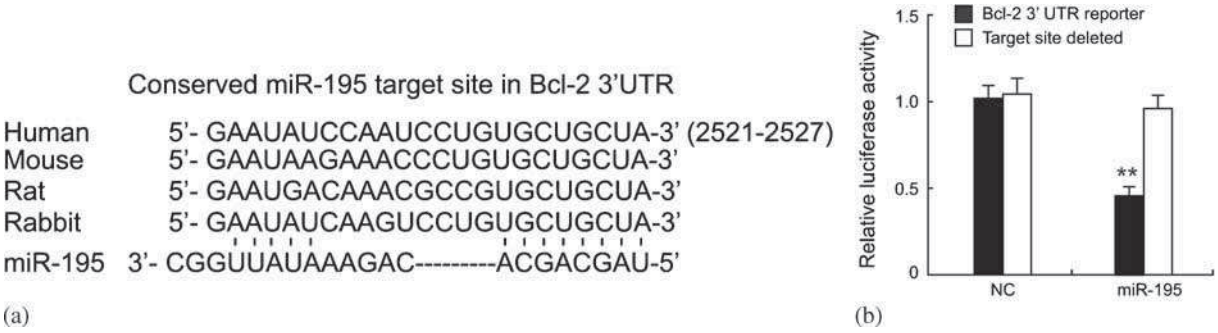

Figure 3. Bcl-2 is a target gene of miR-195. (a) The sequence alignment between miR-195 and Bcl-2 3′-UTR. (b) The luciferase assay results demonstrated that the luciferase activity decreased in miR-195 mimic transfected cardiomyocytes compared with miR-195 NC transfected cardiomyocytes. NC, negative control.

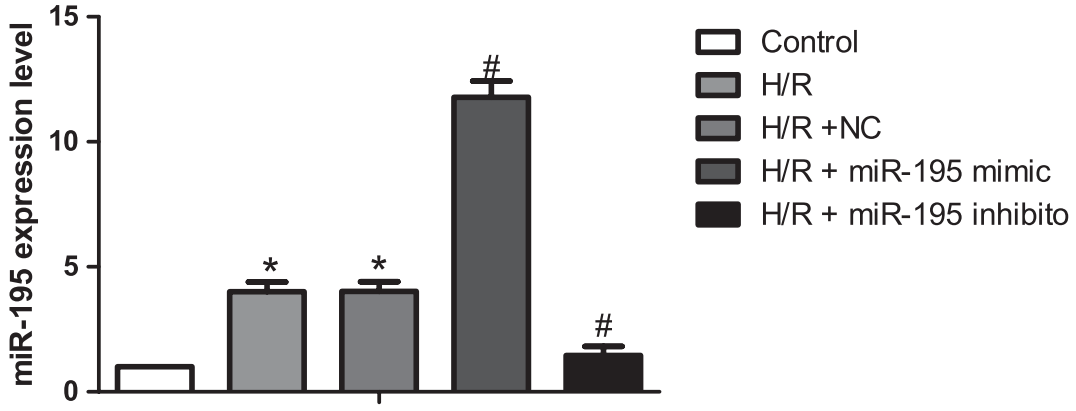

Figure 4. Expression levels of miR-195 in cardiomyocytes of the control group, H/R group, H/R + NC group, H/R + miR-195 mimic group and H/R + miR-195 inhibitor group. NC, negative control; *compared with the control group, $P < 0.05$; #compared with H/R +NC group, $P < 0.05$.

was attenuated by the knock down of miR-195 expression in H/R + miR-195 inhibitor group which was also compared with H/R + NC group ($P < 0.05$).

Bcl-2 and Bax mRNA expression in cardiomyocytes

Compared with the control group, the expression levels of Bcl-2 mRNA decreased significantly in H/R and H/R + NC groups (both $P < 0.05$). No apparent difference existed in Bcl-2 mRNA expression levels between the H/R and H/R + NC groups ($P > 0.05$). Compared with the H/R + NC group, Bcl-2 mRNA expression levels decreased obviously in the H/R + miR-195 mimic group ($P < 0.05$); while Bcl-2 mRNA expression levels increased obviously in the H/R + miR-195 inhibitor group ($P < 0.05$). As for the expression level of Bax mRNA, it increased significantly in H/R and

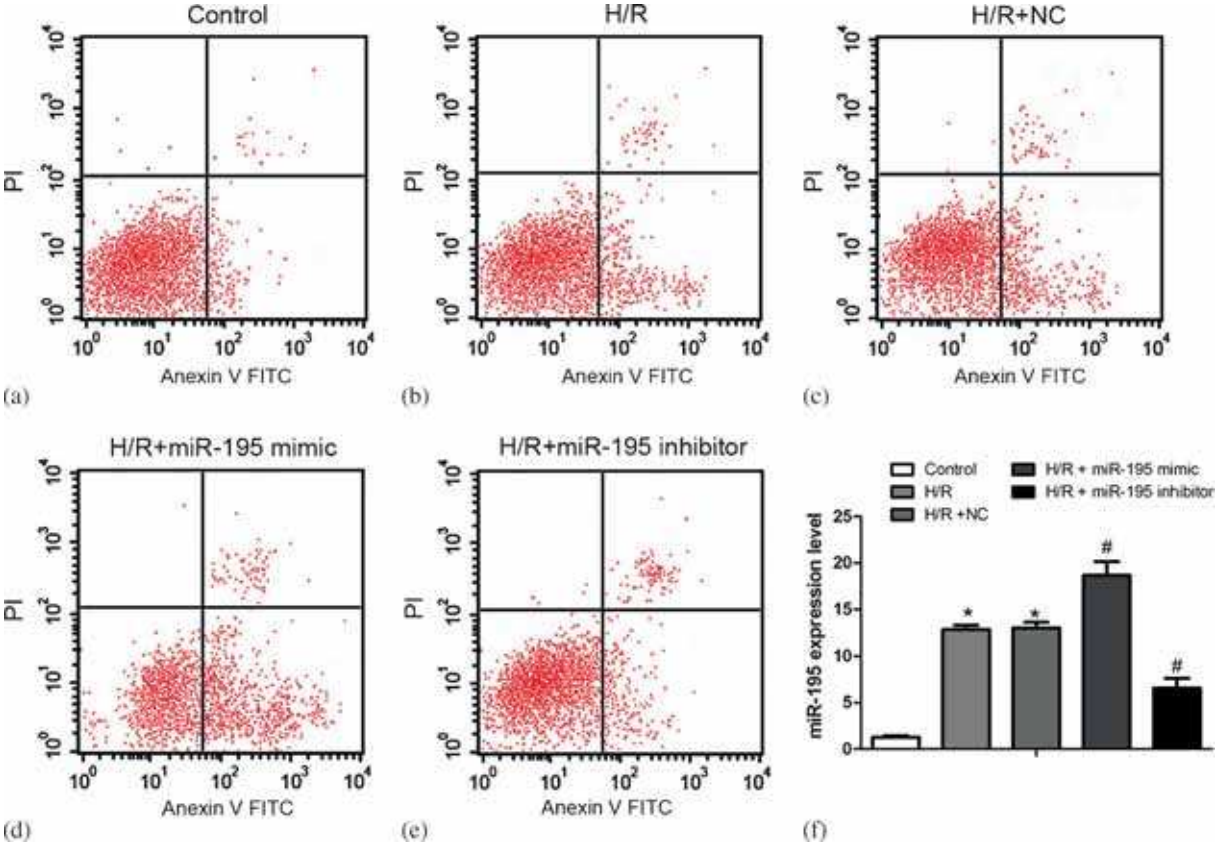

Figure 5. Effects of miR-195 overexpression on cardiomyocytes apoptosis. NC, negative control; *compared with the control group, $P < 0.01$; #compared with the H/R + NC group, $P < 0.01$.

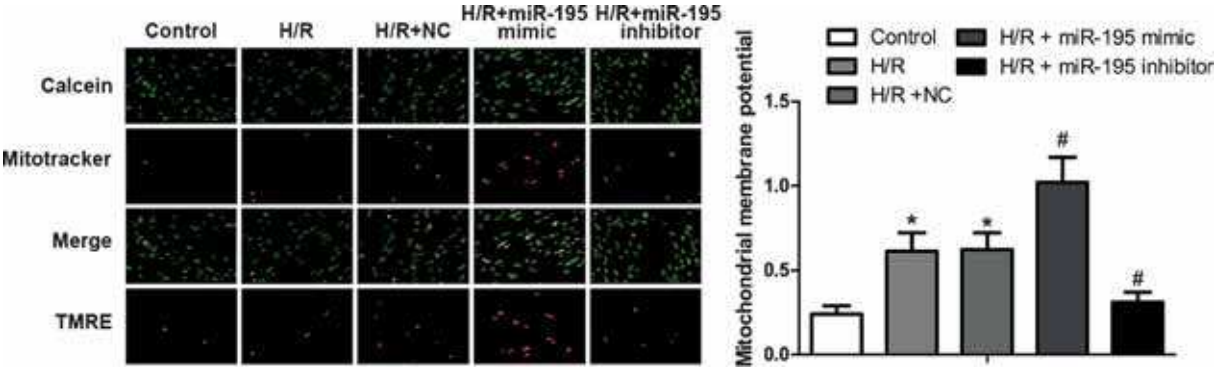

Figure 6. Effects of miR-195 on mitochondrial membrane potential in cardiomyocytes. NC, negative control; *compared with the control group, $P < 0.05$; #compared with the H/R +NC group, $P < 0.05$.

H/R + NC groups as compared to the control group (both $P < 0.05$). Bax mRNA expression level in H/R group showed no obvious difference from that of the H/R + NC group ($P > 0.05$). Compared with the H/R + NC group, Bax mRNA expression levels increased apparently in the H/R + miR-195 mimic group while decreased obviously in the H/R + miR-195 inhibitor group (both $P < 0.05$) (figure 7).

Effect of miR-195 overexpression on Bcl-2, Bax, Cyt-c protein expression

The Bcl-2 protein expression level decreased markedly, while Bax protein expression level increased obviously in H/R and H/R + NC groups as compared with the control group, which was statistically different (all $P < 0.05$) (figure 8). When compared with H/R + NC group, the protein expression of Bcl-2 in H/R + miR-195 mimic group was significantly downregulated, and the Bcl-2 protein expression was obviously increased in H/R + miR-195 inhibitor group; while the protein expression of Bax was upregulated significantly in H/R + miR-195 mimic group and downregulated markedly in the H/R + miR-195 inhibitor group (all $P < 0.05$). The translocation of Cyt-c from mitochondria to the cytoplasm was analysed by testing Cyt-c expression in the cytoplasm. The Cyt-c expression in H/R group and H/R + NC group was upregulated compared with the control group (both $P < 0.05$). Additionally, the Cyt-c expression increased evidently in H/R + miR-195 mimic group while decreased obviously in H/R + miR-195 inhibitor group as compared with the H/R+NC group (both $P < 0.05$).

Activation of caspase-3 and caspase-9 after H/R model construction and miR-195 transfection

In H/R and H/R + NC groups, the activation of caspase-3 and caspase-9 was enhanced in contrast to the control group (both $P < 0.05$) (figure 9). By comparison of H/R + NC group and H/R + miR-195 mimic group, the activation of caspase-3 and caspase-9 was remarkably enhanced in H/R + miR-195 mimic group ($P < 0.05$). Yet, in H/R + miR-195 inhibitor group, the activation of caspase-3 and caspase-9 was attenuated ($P < 0.05$).

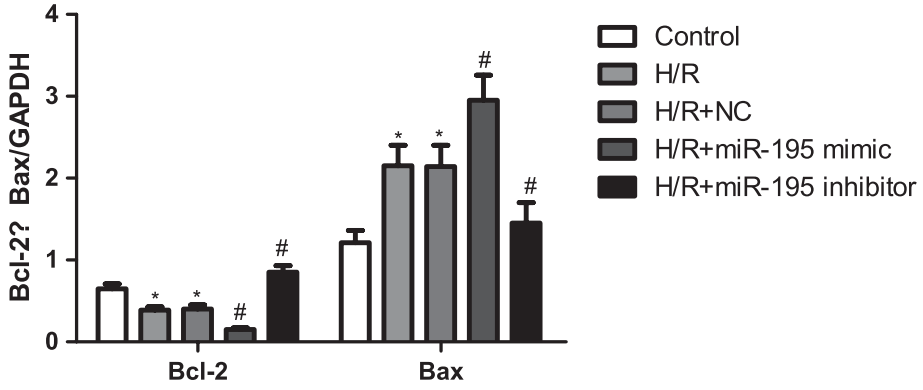

Figure 7. RT-PCR for Bcl-2 and Bax mRNA expression levels in the control group, H/R, H/R + NC, H/R + miR-195 mimic and H/R + miR-195 inhibitor groups. NC, negative control; *compared with the control group, $P < 0.05$; #compared with H/R +NC group, $P < 0.05$.

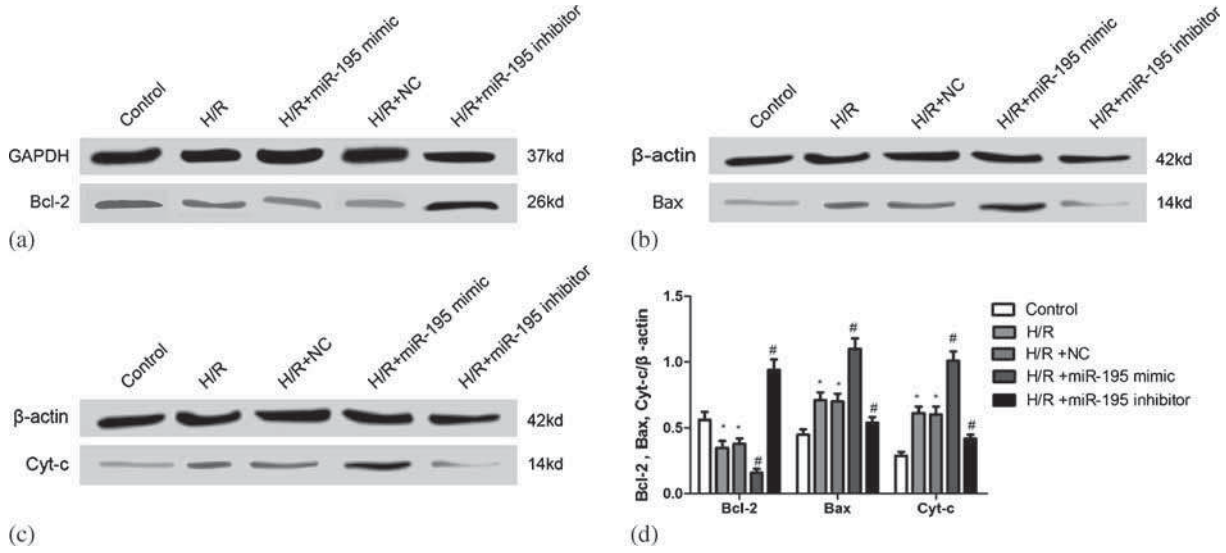

Figure 8. Western blot analysis of Bcl-2, Bax and Cyt-c protein expression levels in cardiomyocytes after transfection. *Compared with the control group, $P < 0.05$. #Compared with H/R + NC group, $P < 0.05$.

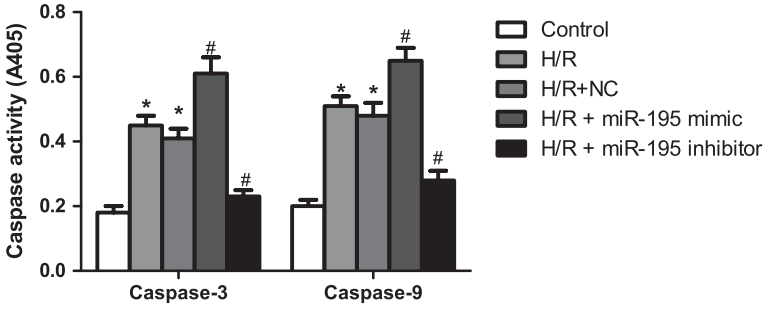

Figure 9. Comparisons of the activation of caspase-3 and caspase-9 among the control, H/R, H/R + NC, H/R + miR-195 mimic and H/R + miR-195 inhibitor groups. NC, negative control; *compared with the control group, $P < 0.054$; #compared with H/R +NC group, $P < 0.05$.

Discussion

MiR-195 is involved in the cell cycle, apoptosis and proliferation by exerting regulatory roles in target proteins (He *et al.* 2011). In our study, cardiomyocyte-specific miR-195 expression was observed to be significantly upregulated nonfatal dilated cardiomyopathy, which was associated with progression of cardiac ischaemia and heart failure (Small *et al.* 2010; Edwards *et al.* 2010). It was documented that the upregulated miR-195 expression induces cardiomyocyte apoptosis by increasing reactive oxygen species (ROS) production to stimulate biological oxidation in cellular activities (Zhu *et al.* 2011). On the other hand, the antimiR-195 inhibitors can effectively knock out and silence miR-195 activity *in vitro*, thus preventing cardiomyocytes from hypoxia-induced cardiomyocyte death and cardiac remodelling in response to ischaemic damage (Hullinger *et al.* 2012). However, the mechanism of miR-195 action has not been completely understood, and the possible explanation is that miR-195 activation regulates the expression of a number of cell cycle genes that are implicated in mitochondrial-related apoptotic pathway, impacting cardiomyocyte survival (Porrello *et al.* 2011). MiR-195 is a member of miR-15 gene family which has been reported by a previous study of Liu *et al.* to be upregulated in response to cardiac I/R injury which indicating that downregulation of miR-15 may be a promising strategy to reduce myocardial apoptosis induced by cardiac I/R injury (Topkara and Mann 2011; Liu *et al.* 2012). In addition, in line with our results, Luo *et al.* (2010) also have found that miR-195 expression in myocardial I/R injuries was upregulated. Cai *et al.* (2010) have reported that the forced miR-195 overexpression in transgenic mice successfully induced cardiac hypertrophic growth and heart failure.

Our present study suggested that Cyt-c expression was evidently increased in H/R + miR-195 mimic group and the activation of caspase-3 and caspase-9 was remarkably enhanced in H/R + miR-195 mimic group. Cardiomyocyte

apoptosis attributes to the activation of mitochondrial apoptotic pathway which is characterized by alteration of mitochondrial permeability and the Cyt-c release into cytoplasm (Parra *et al.* 2008). Mitochondrial membrane potential and Cyt-c distribution are used as indexes of the activation of mitochondrial apoptotic pathway (Parra *et al.* 2008). The mitochondrial stage of apoptosis control is mediated by Bcl-2 activation and the caspase cascade is thereby activated leading to mitochondrial fragmentation and apoptotic susceptibility (Suen *et al.* 2008; Tomasetti *et al.* 2014). The loss of mitochondrial membrane potential take up the calcium, stimulate the leakage of Cyt-c and initiate apoptosis through the opening of permeability transition pores (Wu *et al.* 2010). Subsequently, Cyt-c combines with an inactive initiator caspase, procaspase-9, leading to the activation of caspase-9 and triggering a cascade of caspase (caspase-3, caspase-6 and caspase-7) activation (Kang and Reynolds 2009). Caspase-3 and caspase-9 are the notable effectors in cell apoptosis and their activities were significantly increased to induce cell apoptosis (Miura *et al.* 2008; Zhou *et al.* 2010; Zhu *et al.* 2012). Evidently, the antiapoptotic Bcl-2 plays a great role in inhibiting cell apoptosis by interacting with proapoptotic members and keeping them away from mitochondria, thereby preventing Cyt-c release and production of caspase-3 and caspase-9 (Bienertova-Vasku *et al.* 2013). Also, Perrelli *et al.* (2011) have evidenced that mitochondria and ROS paly significant role in I/R injury and cardioprotective mechanisms (Perrelli *et al.* 2011).

MiR-195 acts as a negative regulator of Bcl-2 through binding to its respective binding site in 3′-UTR of the Bcl-2 mRNA (He *et al.* 2011). Therefore, Bcl-2 is a confirmed target gene of miR-195, and its activation that is involved in miR-195-mediated apoptosis effect is inhibited by miR-195 (He *et al.* 2011). Our study found that Bcl-2 is the target gene of miR-195, and increased miR-195 expression can attenuate miR-195 activation. For example, the role of miR-195 overexpression in tumourigenesis was identified to exert its proapoptotic function through downregulating Bcl-2 expression, suggesting that miR-195 plays vital roles in cancer pathogenesis and cancer therapy (Liu *et al.* 2010). On the other hand, miR-195 was found to be strongly upregulated in I/R hearts and miR-195 overexpression induces cardiomyocyte apoptosis by suppressing antiapoptotic factor Bcl-2 (Ikeda *et al.* 2007; Zhu and Fan 2012). The overexpression of miR-195 in the heart is a big challenge for IHD patients which can enhance myocyte loss and heart failure (van Rooij *et al.* 2006). In the light of these findings, miRNA-195 may be a novel therapeutic target in cardiovascular disorders by designing miRNA inhibitors to manipulate their expression and function (van Rooij and Olson 2012; Maegdefessel 2014). In a previous study of Tang *et al.* (2009), Bcl-2 has also been detected to be a target gene for miRNA-1 functioning in the regulation of cardiomyocyte apoptosis which is involved in posttranscriptional repression of Bcl-2. In a short review, which focussed on the regulation of Bcl-2 family proteins by miRNAs that target multiple Bcl-2, it has been supported the involvement of miRNAs targeting Bcl-2 in the regulation of cerebral ischaemia (Ouyang and Giffard 2014).

In conclusion, the miR-195 expression was upregulated in myocardial I/R injury and miR-195 overexpression may promote cardiomyocyte apoptosis by targeting Bcl-2 and inducing mitochondrial apoptotic pathway. Importantly, miR-195 may be a promising target to reduce cardiomyocyte apoptosis and treat I/R injury.

Acknowledgement

We would like to acknowledge the instructors and work mates for their helpful comments on this paper.

References

Bienertova-Vasku J., Sana J. and Slaby O. 2013 The role of microRNAs in mitochondria in cancer. *Cancer Lett.* **336**, 1–7.

Cai B., Pan Z. and Lu Y. 2010 The roles of microRNAs in heart diseases: a novel important regulator. *Curr. Med. Chem.* **17**, 407–411.

Czabotar P. E., Lessene G., Strasser A. and Adams J. M. 2014 Control of apoptosis by the BCL-2 protein family: implications for physiology and therapy. *Nat. Rev. Mol. Cell Biol.* **15**, 49–63.

Deng H., Guo Y., Song H., Xiao B., Sun W., Liu Z. *et al.* 2013 MicroRNA-195 and microRNA-378 mediate tumor growth suppression by epigenetical regulation in gastric cancer. *Gene* **518**, 351–359.

Di Y., Lei Y., Yu F., Changfeng F., Song W. and Xuming M. 2014 MicroRNAs expression and function in cerebral ischemia reperfusion injury. *J. Mol. Neurosci.* **53**, 242–250.

Diez E. R., Altamirano L. B., Garcia I. M., Mazzei L., Prado N. J., Fornes M. W. *et al.* 2015 Heart remodeling and ischemia-reperfusion arrhythmias linked to myocardial vitamin d receptors deficiency in obstructive nephropathy are reversed by paricalcitol. *J. Cardiovasc. Pharmacol. Ther.* **20**, 211–220.

Dongworth R. K., Mukherjee U. A., Hall A. R., Astin R., Ong S. B., Yao Z. *et al.* 2014 DJ-1 protects against cell death following acute cardiac ischemia-reperfusion injury. *Cell Death Dis.* **5**, e1082.

Edwards J. K., Pasqualini R., Arap W. and Calin G. A. 2010 MicroRNAs and ultraconserved genes as diagnostic markers and therapeutic targets in cancer and cardiovascular diseases. *J. Cardiovasc. Transl. Res.* **3**, 271–279.

Frank A., Bonney M., Bonney S., Weitzel L., Koeppen M. and Eckle T. 2012 Myocardial ischemia reperfusion injury: from basic science to clinical bedside. *Semin. Cardiothorac. Vasc. Anesth.* **16**, 123–132.

Frohlich G. M., Meier P., White S. K., Yellon D. M. and Hausenloy, D. J. 2013 Myocardial reperfusion injury: looking beyond primary PCI. *Eur. Heart J.* **34**, 1714–1722.

Hausenloy D. J. and Yellon D. M. 2013 Myocardial ischemia-reperfusion injury: a neglected therapeutic target. *J. Clin. Invest.* **123**, 92–100.

He J. F., Luo Y. M., Wan X. H. and Jiang D. 2011 Biogenesis of MiRNA-195 and its role in biogenesis, the cell cycle, and apoptosis. *J. Biochem. Mol. Toxicol.* **25**, 404–408.

Hullinger T. G., Montgomery R. L., Seto A. G., Dickinson B. A., Semus H. M., Lynch J. M. *et al.* 2012 Inhibition of miR-15 protects against cardiac ischemic injury. *Circ. Res.* **110**, 71–81.

Ikeda S., Kong S. W., Lu J., Bisping E., Zhang H., Allen P. D. *et al.* 2007 Altered microRNA expression in human heart disease. *Physiol. Genomics* **31**, 367–373.

Jin L. H. and Wei C. 2014 Role of microRNAs in the warburg effect and mitochondrial metabolism in cancer. *Asian Pac. J. Cancer Prev.* **15**, 7015–7019.

Jin Y., Lu J., Wen J., Shen Y. and Wen X. 2015 Regulation of growth of human bladder cancer by miR-192. *Tumour Biol.* **36**, 3791–3797.

Kang M. H. and Reynolds C. P. 2009 Bcl-2 inhibitors: targeting mitochondrial apoptotic pathways in cancer therapy. *Clin. Cancer Res.* **15**, 1126–1132.

Lei H., Tang J., Li H., Zhang H., Lu C., Chen H. *et al.* 2014 MiR-195 affects cell migration and cell proliferation by down-regulating DIEXF in hirschsprung's disease. *BMC Gastroenterol.* **14**, 123.

Liu L., Chen L., Xu Y., Li R. and Du X. 2010 microRNA-195 promotes apoptosis and suppresses tumorigenicity of human colorectal cancer cells. *Biochem. Biophys. Res. Commun.* **400**, 236–240.

Liu L. F., Liang Z., Lv Z. R., Liu X. H., Bai J., Chen J. *et al.* 2012 microRNA-15a/b are up-regulated in response to myocardial ischemia/reperfusion injury. *J. Geriatr. Cardiol.* **9**, 28–32.

Liu Y., Yang H., Song L., Li N., Han Q. Y., Tian C. *et al.* 2014 AGGF1 protects from myocardial ischemia/reperfusion injury by regulating myocardial apoptosis and angiogenesis. *Apoptosis* **19**, 1254–1268.

Luo X., Zhang H., Xiao J. and Wang Z. 2010 Regulation of human cardiac ion channel genes by microRNAs: theoretical perspective and pathophysiological implications. *Cell Physiol. Biochem.* **25**, 571–586.

Maegdefessel L. 2014 The emerging role of microRNAs in cardiovascular disease. *J. Intern. Med.* **276**, 633–644.

Miura T., Chiba M., Kasai K., Nozaka H., Nakamura T., Shoji T. *et al.* 2008 Apple procyanidins induce tumor cell apoptosis through mitochondrial pathway activation of caspase-3. *Carcinogenesis* **29**, 585–593.

Moran A. E., Forouzanfar M. H., Roth G. A., Mensah G. A., Ezzati M., Flaxman A. *et al.* 2014 The global burden of ischemic heart disease in 1990 and 2010: the global burden of disease 2010 study. *Circulation* **129**, 1493–1501.

Ouyang Y. B. and Giffard R. G. 2014 MicroRNAs affect BCL-2 family proteins in the setting of cerebral ischemia. *Neurochem. Int.* **77**, 2–8.

Parra V., Eisner V., Chiong M., Criollo A., Moraga F., Garcia A. *et al.* 2008 Changes in mitochondrial dynamics during ceramide-induced cardiomyocyte early apoptosis. *Cardiovasc. Res.* **77**, 387–397.

Perrelli M. G., Pagliaro P. and Penna C. 2011 Ischemia/reperfusion injury and cardioprotective mechanisms: Role of mitochondria and reactive oxygen species. *World J. Cardiol.* **3**, 186–200.

Pisarenko O., Shulzhenko V., Studneva I., Pelogeykina Y., Timoshin, A., Anesia R. *et al.* 2014 Structural apelin analogues: mitochondrial ROS inhibition and cardiometabolic protection in myocardial ischemia-reperfusion injury. *Br. J. Pharmacol.* **172**, 293–2945.

Porrello E. R., Johnson B. A., Aurora A. B., Simpson E., Nam Y. J., Matkovich S. J. and et al. 2011 MiR-15 family regulates postnatal mitotic arrest of cardiomyocytes. *Circ. Res.* **109**, 670–679.

Qu J., Zhao L., Zhang P., Wang J., Xu N., Mi W. *et al.* 2015 MicroRNA-195 chemosensitizes colon cancer cells to the chemotherapeutic drug doxorubicin by targeting the first binding site of BCL2L2 mRNA. *J. Cell Physiol.* **230**, 535–545.

Siddall H. K., Yellon D. M., Ong S. B., Mukherjee U. A., Burke N., Hall A. R. *et al.* 2013 Loss of PINK1 increases the heart's vulnerability to ischemia-reperfusion injury. *PLoS One* **8**, e62400.

Skommer J., Rana I., Marques F. Z., Zhu W., Du Z. and Charchar F. J. 2014 Small molecules, big effects: the role of microRNAs in regulation of cardiomyocyte death. *Cell Death Dis.* **5**, e1325.

Small E. M., Frost R. J. and Olson E. N. 2010 MicroRNAs add a new dimension to cardiovascular disease. *Circulation* **121**, 1022–1032.

Suen D. F., Norris K. L. and Youle R. J. 2008 Mitochondrial dynamics and apoptosis. *Genes Dev.* **22**, 1577–1590.

Tang Y., Zheng J., Sun Y., Wu Z., Liu Z. and Huang G. 2009 MicroRNA-1 regulates cardiomyocyte apoptosis by targeting Bcl-2. *Int. Heart J.* **50**, 377–387.

Tomasetti M., Neuzil J. and Dong L. 2014 MicroRNAs as regulators of mitochondrial function: role in cancer suppression. *Biochim. Biophys. Acta* **1840**, 1441–1453.

Topkara V. K. and Mann D. L. 2011 Role of microRNAs in cardiac remodeling and heart failure. *Cardiovasc. Drugs Ther.* **25**, 171–182.

van Rooij E. and Olson E. N. 2012 MicroRNA therapeutics for cardiovascular disease: opportunities and obstacles. *Nat. Rev. Drug Discov.* **11**, 860–872.

van Rooij E., Sutherland L. B., Liu N., Williams A. H., McAnally J., Gerard R. D. *et al.* 2006 A signature pattern of stress-responsive microRNAs that can evoke cardiac hypertrophy and heart failure. *Proc. Natl. Acad. Sci. USA* **103**, 18255–18260.

Wang R., Zhao N., Li S., Fang J. H., Chen M. X., Yang J. *et al.* 2013 MicroRNA-195 suppresses angiogenesis and metastasis of hepatocellular carcinoma by inhibiting the expression of VEGF, VAV2, and CDC42. *Hepatology* **58**, 642–653.

Wu S. H., Hang L. W., Yang J. S., Chen H. Y., Lin H. Y., Chiang J. H. *et al.* 2010 Curcumin induces apoptosis in human non-small cell lung cancer NCI-H460 cells through ER stress and caspase cascade- and mitochondria-dependent pathways. *Anticancer Res.* **30**, 2125–2133.

Yang Y., Li M., Chang S., Wang L., Song T., Gao L. *et al.* 2014 MicroRNA-195 acts as a tumor suppressor by directly targeting Wnt3a in HepG2 hepatocellular carcinoma cells. *Mol. Med. Rep.* **10**, 2643–2648.

Yongchun Z., Linwei T., Xicai W., Lianhua Y., Guangqiang Z., Ming Y. *et al.* 2014 MicroRNA-195 inhibits non-small cell lung cancer cell proliferation, migration and invasion by targeting MYB. *Cancer Lett.* **347**, 65–74.

Zhao F. L., Dou Y. C., Wang X. F., Han D. C., Lv Z. G., Ge S. L. *et al.* 2014 Serum microRNA-195 is down-regulated in breast cancer: a potential marker for the diagnosis of breast cancer. *Mol. Biol. Rep.* **41**, 5913–5922.

Zhou X., Zhang J., Jia Q., Ren Y., Wang Y., Shi L. *et al.* 2010 Reduction of miR-21 induces glioma cell apoptosis via activating caspase 9 and 3. *Oncol. Rep.* **24**, 195–201.

Zhu H. and Fan G. C. 2012 Role of microRNAs in the reperfused myocardium towards post-infarct remodelling. *Cardiovasc. Res.* **94**, 284–292.

Zhu H., Yang Y., Wang Y., Li J., Schiller P. W. and Peng T. 2011 MicroRNA-195 promotes palmitate-induced apoptosis in cardiomyocytes by down-regulating Sirt1. *Cardiovasc. Res.* **92**, 75–84.

Zhu L., Yuan H., Guo C., Lu Y., Deng S., Yang Y. *et al.* 2012 Zearalenone induces apoptosis and necrosis in porcine granulosa cells via a caspase-3- and caspase-9-dependent mitochondrial signaling pathway. *J. Cell Physiol.* **227**, 1814–1820.

Received 8 April 2015, in revised form 26 June 2015; accepted 24 July 2015
Unedited version published online: 28 July 2015
Final version published online: 18 February 2016